Coherence between Internal and External Noise Generated by a Gas Turbine Combustor

Warren C. Strahle,* M. Muthukrishnan,† and Douglas H. Neale‡
Georgia Institute of Technology, Atlanta, Ga.

Experiments and analysis on a gas turbine combustor unit are reported with a view in mind to separate propagated acoustic power from nonpropagating "pseudosound." Analytically, it is suggested that a transition frequency will exist below which the interior pressure fluctuations are nonpropagating, whereas above this frequency, of the order of 100 Hz, the noise is dominated by propagating acoustic waves. Coherence measurements are reported which show this concept to be borne out experimentally. Coherence between interior and exterior microphones is measured over a range of experimental conditions for a gas turbine combustor exhausting directly to the atmosphere. The purpose is to show that below a certain frequency, measurements of interior noise are not indicative of combustion noise ultimately propagating from an engine.

Nomenclature

a = combustor radius
c = speed of sound
D = denominator defined by Eqs. (15)
e = specific sensible internal energy
F = transverse tail of series defined by Eq. (17)
f = defined by Eq. (11)
G_{ij} = cross power spectrum between signals i and j
i = $(-1)^{1/2}$
J_m = Bessel function of mth order
k = wavenumber defined by Eqs. (15)
l = length of combustor
M = Mach number
p = pressure
$\dot{Q}$ = heat release rate per unit volume
r = radial coordinate
S = cross-section area
t = time
u = axial velocity component
V = can volume
v = vector velocity
x = axial coordinate measured from the upstream end of the combustor
β = specific acoustic admittance
$\mathcal{K}$ = eigenvalue defined by Eqs. (15)
$\mathcal{E}$ = constant defined by Eqs. (15)
γ = ratio of specific heats
Λ = constant defined by Eqs. (15)
ψ = transverse eigenfunction defined by Eqs. (15)
η = defined by Eqs. (15)
ρ = density
θ = angular coordinate
ω = frequency
$\theta[\ ]$ = of the order of

Subscripts

a = acoustic (dilatational) quantity
e = combustor exit plane
mn = summation indices for transverse modes
o = dummy integration variable
v = vortical (turbulent) quantity
w = side walls of the combustor
ω = Fourier transform

Superscripts

$\sim$ = dimensional quantity
$\bar{}$ = time mean quantities or ensemble average of statistical quantities
σ = summation index for transverse modes
$'$ = perturbation quantities

Received Jan. 6, 1977; presented as Paper 77-20 at the AIAA 15th Aerospace Sciences Meeting, Los Angeles, Calif., Jan. 24-26, 1977; revision received April 8, 1977.

Index categories: Aircraft Noise, Powerplant; Airbreathing Engine Testing.

*Regents' Professor, School of Aerospace Engineering. Associate Fellow AIAA.

†Graduate Research Assistant, School of Aerospace Engineering.

‡Research Engineer, School of Aerospace Engineering. Member AIAA.

Introduction

IT is reasonably well understood that in order for noise generated interior to a turbopropulsion system to propagate to the surroundings, a dilatation wave must accompany this noise. That is, in order for a propagational wave, which carries acoustic energy, to be present, the divergence of the velocity vector must be nonzero. Alternatively, some of the interior noise is caused by vortical motions of the turbulence which are local in nature, not propagational. This problem of "pseudosound" coexisting with propagational noise causes difficulties in interpreting interior microphone measurements insofar as their connection with the ultimately radiated sound is concerned. Nevertheless, one of the primary techniques used to investigate the existence of "core engine noise" or "excess noise" has been the comparison of interior and exterior microphone measurements.[1-3]

A technique used previously[1,3] to detect a casual relationship between an interior and exterior microphone has been the cross-correlation function. The use of this function in interpretation of the results requires exact specification of the two functions which are directly proportional to each other. So, for example, the interior pressure and the time derivative of the pressure were cross-correlated with the far-field pressure in Ref. 3 to determine which of the two functions was related in direct proportion to the far-field pressure. A less specific but powerful function to investigate a linear, causal relation between two variables is the coherence function.[4] It has the property that if two variables are related by a linear transform operation it will be unity, regardless of the transform operation. It will be zero if there is no causal relationship. This behavior occurs regardless of the transform operation. For example, in Ref. 3 the coherence function between either the time derivative of the interior pressure or the pressure itself and the far-field pressure would be unity if *either* of the two quantities were perfectly correlated with the

far-field pressure because differentiation is a linear transform operation. The coherence function will be used in this paper to determine the frequency regimes, if any, in which there is a linear causal relation between interior and exterior pressure fluctuations.

The purposes of this paper are two-fold. First, it will be analytically established that below a certain frequency (apparatus dependent) the hydrodynamic noise generated by turbulence within a combustor is nonpropagational and consequently incoherent with exterior sound measurements. Secondly, for a particular experimental set-up, this fact will be demonstrated.

Analysis

The theory of combustion noise for the gas turbine combustor will assume that the fluid mechanics process is one of the gas phase alone. Therefore, the complications of fuel evaporation and mass, momentum and energy transfer between liquid and gas phases are avoided. Consideration of these processes is not necessary for an adequate understanding of combustion noise generation, since the dominant noise generation process is a gas phase one – the unsteady heat release in the turbulent gas phase. Although mass release fluctuations in space and time by evaporation from the spray droplets would indeed cause some noise, order-of-magnitude arguments support the contention that the extreme heat release involved causes greater local fluctuations in gas velocity, the primary source of noise. The approach will be to study the behavior of the fluctuating components of various field quantities about their time-mean values. These fluctuations will contain both the turbulence and acoustic fluctuations, and a split into vortical turbulent motions and acoustic quantities is found possible by the method below.

Molecular transport processes are neglected in comparison with turbulent transport. Although it would be necessary to consider these to recover exact flame structure (since the actual combustion process must take place in the microscale of the turbulence), the flame structure is basically left as an unknown in the following treatment, to be determined by knowledge of both the time-mean field quantities and the fluctuation quantities.

The equations of continuity, momentum, energy, and state for an inviscid perfect gas are

$$\frac{\partial\tilde{\rho}}{\partial\tilde{t}} + \tilde{\nabla}\cdot(\tilde{\rho}\tilde{v}) = 0, \quad \frac{\partial\tilde{v}}{\partial\tilde{t}} + \tilde{v}\cdot\tilde{\nabla}\tilde{v} = -\frac{\tilde{\nabla}\tilde{p}}{\tilde{\rho}} \tag{1a}$$

$$\frac{\tilde{D}\tilde{e}}{\tilde{D}\tilde{t}} + \tilde{p}\frac{\tilde{D}(1/\tilde{\rho})}{\tilde{D}\tilde{t}} = \frac{\tilde{\dot{Q}}}{\tilde{\rho}}, \quad \frac{\tilde{p}}{\tilde{\rho}} = (\gamma-1)\tilde{e} \tag{1b}$$

Nondimensionalizing Eqs. (1) by the can length, the exit plane mean speed of sound, density, and pressure, the conservation equations become

$$\frac{\partial\rho}{\partial t} + \nabla\cdot(\rho v) = 0 \tag{2}$$

$$\frac{\partial v}{\partial t} + v\cdot\nabla v = -\frac{\nabla p}{\gamma\rho} \tag{3}$$

$$\frac{Dp}{Dt} - \gamma\frac{p}{\rho}\frac{D\rho}{Dt} = (\gamma-1)\dot{Q} \tag{4}$$

Constructing the time mean equation the usual results are found. That is, the pressure gradient is of the order of the square of the Mach number so that if $M^2 << 1$, $\bar{p}\approx 1$; furthermore, the primary effect of $\dot{Q}$ is to cause a dilation of the velocity vector, not a strong pressure change. These remarks presume well-distributed combustion throughout the combustor so that $\nabla\cdot\bar{v}$ is of the order of unity throughout the combustor. This is generally true for a spray type diffusion flame.

Now consider the *linearized* fluctuation equations. By linearization all processes in the turbulence relying on nonlinearities such as generation, spectral transfer, and decay (which is not considered because viscosity is not considered) are omitted. Consideration is therefore focused on the energy containing eddies over the can length which is presumed short compared with a length required for a substantial alteration of the turbulence structures. Combining Eqs. (2) and (4), Eqs. (3) and (4) become after linearization

$$\frac{\partial v'}{\partial t} + \nabla(\bar{v}\cdot v') + \nabla\times\bar{v}\times v' + \nabla\times\bar{v} = -\frac{\nabla p'}{\gamma\bar{\rho}} \tag{5}$$

$$\frac{\partial p'}{\partial t} + v'\cdot\nabla\bar{p} + \bar{v}\cdot\nabla p' + \gamma p'\nabla\cdot\bar{v} + \gamma\bar{p}\nabla\cdot v' = (\gamma-1)\dot{Q}' \tag{6}$$

In Eq. (6) the second term may be dropped because $\nabla\bar{p}$ is $\theta(M^2)$ and in the fifth term $\bar{p}=1$ may be used, correct to terms of $\theta(M^2)$ compared to unity. Now let the perturbation velocity vector be split into its lamellar and solenoidal components.

$$v' = v_a' + v_v'$$

where $\nabla\cdot v_v' = \nabla\times v_a' = 0$. Here v_a' is associated with a dilatational acoustic motion and v_v' is associated with vortical turbulent motions convected by the mean fluid motion. Because of the linearity of Eqs. (5) and (6) the pressure may be considered as split into two components p_a' and p_v' and Eqs. (5) and (6) may be split as follows:

$$\frac{\partial v_a'}{\partial t} + \nabla(\bar{v}\cdot v_a') + \nabla\times\bar{v}\times v_a' = -\frac{\nabla p_a'}{\gamma\bar{\rho}} \tag{7}$$

$$\frac{\partial p_a'}{\partial t} + \bar{v}\cdot\nabla p_a' + \gamma p_a'\nabla\cdot\bar{v} + \gamma\nabla\cdot v_a' = (\gamma-1)\dot{Q}' \tag{8}$$

$$\frac{\partial p_v'}{\partial t} + \bar{v}\cdot\nabla p_v' = \frac{\bar{D}}{Dt}p_v' = -\gamma p_v'\nabla\cdot\bar{v} \tag{9}$$

$$\frac{\partial v_v'}{\partial t} + \nabla(\bar{v}\cdot v_v') + \nabla\times\bar{v}\times v_v' + \nabla\times v_v'\times\bar{v} = -\frac{\nabla p_v'}{\gamma\bar{\rho}} \tag{10}$$

In Eq. (8) $\dot{Q}'$ has been associated with the acoustic problem since heat release per unit volume can produce no torque, only dilatation. In Eq. (9) the expected result is present that the pressure fluctuations produced by the vortical motion are convected by the mean flow, modified only by the right hand side of Eq. (9). If terms of the order of the Mach number are neglected, compared with unity, the second and third terms of Eqs. (7) and (8) may be neglected if $\partial/\partial t$ *is* $\theta(1)$ so that wavelengths are of the order of the combustor length. This assures that the ∇ operator is of order unity. In this case, taking the Fourier transform of Eqs. (7) and (8) and combining

$$\nabla^2 P_{a_\omega} + \omega^2 P_{a_\omega} = -\left.\frac{\partial\dot{Q}}{\partial t}\right)_\omega (\gamma-1) \equiv -f_\omega \tag{11}$$

Equation (11) is an inhomogeneous Helmholtz equation driven by the fluctuating heat release. Furthermore, the source term is the local Eulerian time derivative of the heat release as has occurred previously,[5] not the total time derivative as in the formulation of Ref. 6.

At low values of the frequency, Eq. (11) is not accurate and the primary information comes from Eq. (8) as

$$\gamma\nabla\cdot v_a' = (\gamma-1)\dot{Q}' \tag{12}$$

neglecting terms of $\theta(M)$ compared to unity. The pressure is then determined by Eq. (7) without the time derivative term. Equations (11) and (12) are limiting forms of Eqs. (7) and (8)

at ω of θ (1) and $\omega \to 0$, respectively. Integrating Eq. (12) over the combustor volume and assuming a high impedance head end and walls of the combustor, the Fourier transform of the result yields

$$\int_{S_e} v_{a_{\omega_n}} \mathrm{d}S = \frac{\gamma - 1}{\gamma} \int_V \dot{Q}_\omega \mathrm{d}V \tag{13}$$

Eq. (13) states that the average normal velocity fluctuation at the can exit plane is directly caused by the sum of the heat release fluctuations interior to the can. The average velocity fluctuation at the can exit will radiate sound in accordance with the impedance relation of Ref. 7. In the limit of low frequency and just outside the can

$$p_\omega \propto \omega \int_{S_e} v_{\omega_n} \mathrm{d}S \propto \omega \int_V \dot{Q}_\omega \mathrm{d}V$$

$$p_\omega \to 0 \quad \text{as} \quad \omega \to 0$$

Consequently, since $\dot{Q}_\omega$ must remain bounded if $\omega \to 0$ (by definition of a fluctuating quantity) an observed experimental fact of very low exterior pressure fluctuations at low frequency is recovered analytically. However, it will be seen experimentally that at low frequency the interior pressure fluctuations remain high while the exit plane fluctuations disappear. An interior microphone will see both p_v' and p_a' whereas exterior microphones will only see the effects of p_a', it being a propagational wave containing fluid dilatation. One can therefore expect a possibility that below a certain frequency, if p_a' dominates p_v' at higher frequency, p_v' may dominate p_a'. This is only a possibility analytically because both p_v' and p_a' must remain bounded as $\omega \to 0$ but the end plane impedance relation might drive p_a' to zero faster than p_v'. Any dominance of p_a' at any frequency must come from the source $\dot{Q}'$, and at ω of θ (1) Eq. (11) is the dominant equation if the source is strong enough. Experimentally it is known that propagational sound, called combustion noise, is heard from combustors, and, consequently, there is a frequency regime where Eq. (11) is valid. The point is that *in the limit of low frequency there is no reason to expect a correlation between an interior pressure measurement and the pressure measurement outside the can.* At sufficiently low frequency there is the possibility that nonpropagating "pseudosound" will dominate interior pressure measurements.

Because the exact nature of the turbulence field is not known, it is impossible to state the exact value of ω at which a transition will occur from Eqs. (9) and (10) to Eqs. (7) and (8) as the governing system. This will have to be determined experimentally. The transition will be called the hydrodynamic-to-acoustic transition since Eq. (11) has wave phenomena clearly associated with it while Eqs. (9) and (10) are controlled by the turbulence field. Consider, then, the solution of Eq. (11). To solve Eq. (11) the acoustic behavior of the liner walls and exit plane must be known. From the work of Ref. 7 it is known that the acoustic impedance of the exit plane should differ little from that of an unflanged pipe, open to the infinite surroundings. From the work of Ref. 8 the head end should behave basically as a hard wall. The side walls present a complex acoustic picture, however. It is known experimentally that only weak can resonances appear, so that the side walls must be reasonably absorbent, acoustically. An acoustic admittance, β_w, will be assigned to the side walls which will be left as a free parameter. The magnitude of β_w can be deduced approximately by a comparison of the theoretical and experimental resonance peak heights in the pressure. Under the approximations leading to Eq. (11), therefore, the boundary conditions on p_ω are (assuming a cylindrical combustor)

$$x = 0 \quad \frac{\partial p_\omega}{\partial x} = 0 \tag{14a}$$

$$r = a \quad \frac{\partial p_\omega}{\partial r} + i\omega\beta_w p_\omega = 0 \tag{14b}$$

$$x = l \quad \frac{\partial p_\omega}{\partial x} + i\omega\beta_e p_\omega = 0 \tag{14c}$$

where a is the can radius and $\beta_e = \tilde{u}_{\omega_e}\tilde{\rho}_e\tilde{c}_e/\tilde{p}_{\tilde{\omega}_e}$ is the specific acoustic admittance of the exit plane.

The solution to Eq. (11) subject to Eqs. (14) may be worked out by standard methods, by expansion in terms of normal modes of the combustor. Since $\dot{Q}_\omega$ is a random function of position in the combustor can there are no symmetries that may be invoked to simplify the solution and the solution will contain both symmetric and antisymmetric modes. Since interest is ultimately in comparing a wall-measured pressure against the exterior radiated pressure, the solution is here given for a wall pressure. The solution is

$$p_\omega(x,a,\theta) = \sum_{\substack{m,n=0 \\ \sigma=+1,-1}}^{\infty} (p^\sigma_{\omega_{mn,1}} + p^\sigma_{\omega_{mn,2}}) = p_{\omega_1} + p_{\omega_2}$$

$$p^\sigma_{\omega_{mn,1}} = \frac{\psi^\sigma_{mn}(a,\theta)\left[e^{ik_{mn}(l-x)} + \eta_{mn}e^{-ik_{mn}(l-x)}\right]}{iSk_{mn}\Lambda_{mn}D_{mn}} \cdot \int_0^x \mathrm{d}x_o \cos k_{mn}x_o \int_S \mathrm{d}S_o f_\omega(x_o,r_o,\theta_o)\psi^\sigma_{mn}(r_o,\theta_o)$$

$$p\omega^\sigma_{mn,2} = \frac{\psi^\sigma_{mn}(a,\theta)\cos k_{mn}x}{iSk_{mn}\Lambda_{mn}D_{mn}} \cdot \int_x^l \mathrm{d}x_o \left[e^{ik_{mn}(l-x_o)} + \eta_{mn}e^{-ik_{mn}(l-x_o)}\right] \int_S \mathrm{d}S_o f_\omega \psi^\sigma_{mn}$$

$$k_{mn}^2 = \omega^2 - \mathcal{K}_{mn}^2$$

$$\mathcal{K}_{mn}J'_m(\mathcal{K}_{mn}a) = -i\omega\beta_w J_m(\mathcal{K}_{mn}a)$$

$$\psi^\sigma_{mn} = J_m(\mathcal{K}_{mn}r)\begin{cases}\cos m\theta \\ \sin m\theta\end{cases}\begin{matrix}\sigma=+1 \\ \sigma=-1\end{matrix}$$

$$D_{mn} = e^{ik_{mn}} - \eta_{mn}e^{-ik_{mn}}$$

$$S = \pi a^2$$

$$\eta_{mn} = \left(1 - \frac{\omega\beta_{e_{mn}}}{k_{mn}}\right)\Big/\left(1 + \frac{\omega\beta_{e_{mn}}}{k_{mn}}\right)$$

$$\Lambda_{mn} = \varepsilon_m\left[1 - \frac{m^2 + (\beta_{w_{mn}}\omega a)^2}{(\mathcal{K}_{mn}a)^2}\right]J_m^2(\mathcal{K}_{mn}a)$$

$$\varepsilon = 1 \quad m = 0, \qquad \varepsilon = 1/2 \quad m > 0 \tag{15}$$

The p_{ω_1} part of the solution contains the contribution of f_ω from $x = 0$ to x and p_{ω_2} contains the contributions from x (the measuring point) to 1. The first term in the overall sum ($m = n = 0$, $\sigma = +1$) is the (nearly) plane wave mode. It is not absolutely plane because $\mathcal{K}_{oo} \neq 0$, but is calculated for small $|\mathcal{K}_{oo}a|$ from the Bessel function equation to be

$$\mathcal{K}_{oo} = \left(\frac{2i\omega\beta_{w_{oo}}}{a}\right)^{1/2} \quad [\,|\mathcal{K}_{oo}a| << 1] \tag{16}$$

For practical purposes, however, little error is made in the use of Eq. (16) for $|\mathcal{K}_{oo}a|$ as large as unity. The finite magnitude of $\mathcal{K}_{oo}$ means that

$$\psi^l_{oo} = J_o(\mathcal{K}_{oo}r) \neq 1$$

has a radial dependence, and, consequently, $p^l_{\omega_{oo}}$ has a radial dependence which keeps it from purely plane behavior.

For β_e large, as it is at low ω, $\eta_{oo} \approx -1$, and D_{oo} has a minimum near $\omega = \pi/2$, the quarter wave resonance point.

Thus, a maximum occurs in $p^{\,l}_{\omega_{oo}}$ at the quarter wave frequency, as expected. Because each term in the sum contains a different functional weighting of f_ω in the integrations, each term in the sum is partially incoherent in phase with the other, unless, of course, f_ω is not random in position, which is not to be expected. p_ω may also be represented by

$$p_\omega = p_{\omega_{oo,1}} + p_{\omega_{oo,2}} + F \tag{17}$$

where all three quantities are incoherent with each other and F is the entire transverse mode tail of the doubly infinite series. It would be nice if it could be shown that some of the terms of Eq. (17) could be neglected. Clearly, if $f_\omega = 0$ between x and 1, $p_{\omega_{oo,2}} = 0$. Additionally, if f_ω is nonzero for only a short axial distance near $x = 0$ and ω is low, a careful inspection of Eqs. (15) shows the anticipated behavior that all transverse modes are cutoff ($F \approx 0$) if the measuring point is suffiently far downstream. This latter case cannot be expected to occur in practice since at best one half of the can length must contain active combustion. On the other hand, there is a reasonable expectation that near the quarter wave resonance point the plane wave mode, $p_{\omega_{oo,1 \text{ and } 2}}$, will dominate F. Furthermore, in the limit of small $\omega(\omega \to 0)$ the plane wave mode will dominate F if β_w is small because of the appearance of $k_{oo} \approx \omega$ in the denominator. On the other hand, it should be recalled that at sufficiently low ω, Eq. (11) ceases to be valid. Consequently, numerical calculations are in order to determine the actual magnitudes of various terms.

To experimentally determine whether or not any terms may be neglected in Eq. (17), however, the coherence function may be used.[4] Consider a measurement of the pressure at two combustor position, x and 1. The cross power spectrum of these two pressures is

$$G_{x1} \equiv p_\omega(x) p^*_\omega(1)$$

where the * denotes a complex conjugate. Here

$$p_\omega(1) = p^{\,l}_{\omega_{oo,1}}(1) + F(1)$$

Now note that part of $p^{\,l}_{\omega_{oo,1}}(1)$ contains $p\omega_{oo,1}(x)$ in the integration of Eqs. (15). In fact $p_\omega{}^{l}{}_{oo,1}(1) = H(\omega) p_\omega{}^{l}{}_{oo,1}(x) + J$ where $H(\omega)$ is a linear determined transfer function and J is a frequency dependent random function which is incoherent with any other term. Consequently, let $p^{\,l}_{\omega_{oo,1}}(x) \equiv b$ and the pressures take the form

$$p_\omega(1) = Hb + K$$

$$p_\omega(x) = b + L$$

where K and L are incoherent with b. If a many sample average is taken of G_{x1} to yield $\bar{G}_{x1}$ there results

$$\bar{G}_{x1} = \overline{b\, b^*\, H^*}$$

The auto spectra after averaging are

$$\bar{G}_{xx} = \overline{b\, b^*} + \overline{L\, L^*}$$

$$\bar{G}_{11} = \overline{b\, b^*}\, H\, H^* + \overline{K\, K^*}$$

The coherence function is defined by

$$\gamma^2 = \frac{\bar{G}_{x1} \bar{G}^*_{x1}}{\bar{G}_{xx} \bar{G}_{11}}$$

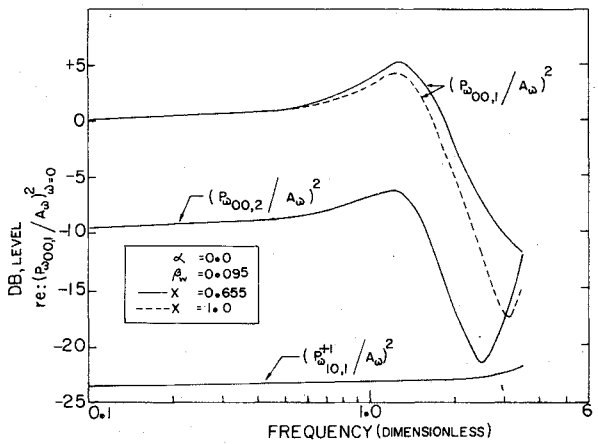

Fig. 1 Relative magnitudes of various mode strengths at various combustor positions for a given combustion noise source strength.

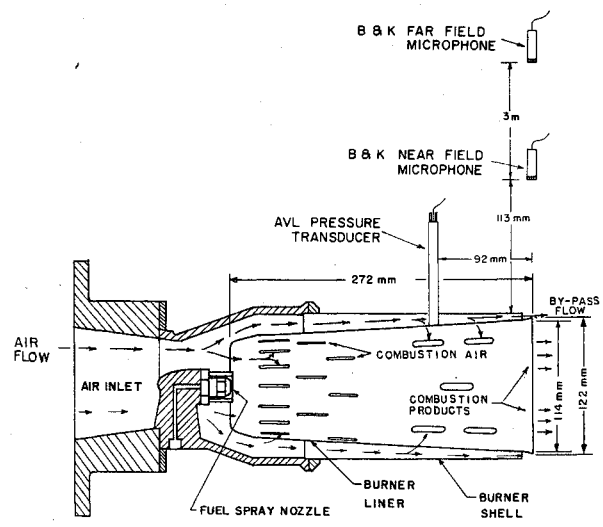

Fig. 2 Schematic of experimental setup.

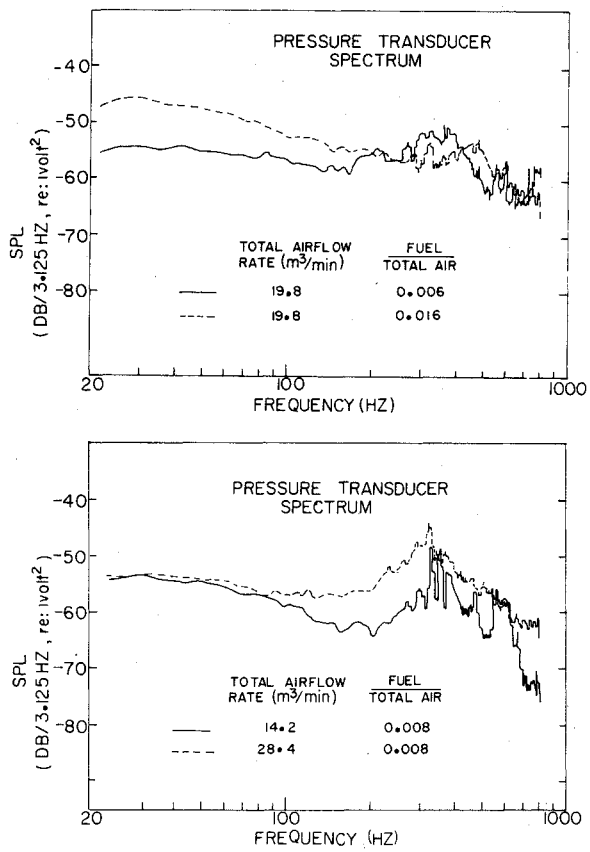

Fig. 3 Interior microphone spectra as functions of airflow rate and fuel/total air. The fraction of air bypassed is approximately 26%.

and there results

$$\gamma^2 = \frac{\overline{bb^{*2}HH^*}}{(\overline{bb^*} + \overline{LL^*})(\overline{bb^*H}\,\overline{H^*} + \overline{KK^*})} \tag{18}$$

If either a) events between x and 1 dominate p_ω behavior (J and L are large so that K and L are large compared with b), or b) F is dominant and $F(1)$ is incoherent with $F(x)$, γ^2 is small. On the other hand if b is the dominant term $\gamma^2 \to 1$. A coherence function of unity (or near unity) in a given frequency range will therefore show that a single term dominates the solution of Eqs. (15) and that events between x and 1 are unimportant ($f_\omega \approx 0$). Furthermore, the coherence function will also show where Eqs. (7) and (8) take over from Eqs. (9) and (10). This can be seen if the microphone at x is dominated by p_v' and the $x=1$ microphone is placed slightly outside of the combustor end plane to sense only propagational sound, p_a'.

If a frequency band is found where $\gamma^2 \approx 1$, it is assumed that $f_\omega \approx 0$ between x and 1. Any deviation from $\gamma^2 \approx 1$ at higher frequencies must then indicate the transverse modes competing with the plane wave mode. Calculations have been performed on Eqs. (15) to compare the magnitudes of $p^I_{\omega_{00}}(x)$ and $p^{\pm 1}_{\omega_{10}}(x)$. A β_m magnitude has been chosen to give roughly the quarter wave resonance peak magnitude which is experimentally observed. β_w has been assumed real, on the basis of no other information. In the calculation, $\psi^I_{00}(a,\theta) = 1$ and $\mathcal{K}_{10}$ real ($\beta_{w_{10}} = 0$) have been assumed for the order-of-magnitude calculations. The position x has been chosen, to correspond with the experimental setup. The expression for β_e is the low frequency asymptotic expression of Levine-Schwinger[9]

$$\beta_e = 1/[\omega a(0.6i + 0.25\omega a)]$$

This has also been used for the first transverse mode calculation. The elimination of the wall damping in the transverse mode calculation will raise its magnitude compared with the case of damping; consequently, this is a conservative comparison of the dominance of the plane wave mode over the transverse mode. The integrals in Eqs. (15) have been estimated by a) carrying out the x_o integration as though f_ω were independent of x_o and b) the transverse integrations have been estimated as

$$\int_S dS_o f_\omega \psi^o_{mn} \equiv A_\omega \left[\frac{1}{S}\int_S \psi^o_{mn}\, dS\right]^{1/2} S$$

where A_ω is an average (unknown) source strength. Shown in Fig. 1 are calculations for the plane wave mode and the first antisymmetric transverse mode (1,0), which is the first transverse mode to cut on as frequency rises. Starting from top to bottom, the plane wave mode at $x=0.655$ with source contributions from 0 to x (00,1) is the dominant term. It shows the quarter wave resonance near $\omega = \pi/2$. Slightly lower in magnitude is the plane wave mode evaluated at $x=1$, now using the source contribution from $x=0$ to $x=1$. The reason it is slightly lower in magnitude, even though the source contributes over the full can length, is that the impedance condition at the can exit plane requires nearly constant pressure, whereas there is no such restriction interior to the combustor. Much lower in magnitude is the plane wave contribution to the $x=0.655$ position from the combustor position downstream of the transducer position (00,2). Consequently, even if the combustor source strength were as large downstream as upstream of the transducer position it would not contribute to the transducer measurement. Finally, well down from the plane wave modes, is the first transverse mode contribution. It is almost completely cut off at the transducer location over the frequency range shown. Theoretically, it would cut on completely at a dimensionless frequency of 8.8. The frequencies of interest experimentally are well below this value so that the F function of Eq. (17) may indeed be neglected. The major conclusion, therefore, is that in Eq. (18) $\gamma^2 = 1$ should result over the frequency range of interest as long as the frequency is high enough that Eqs. (15) are a valid solution to the problem.

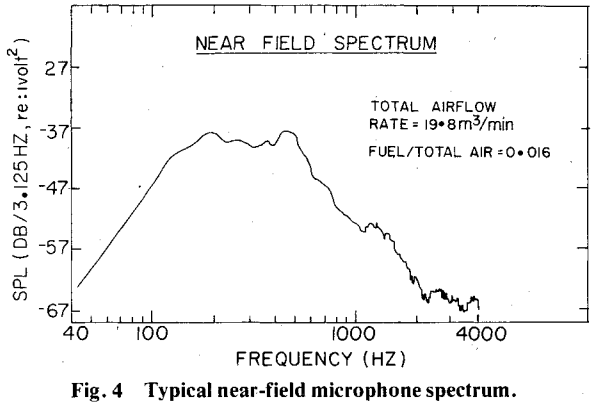

Fig. 4 Typical near-field microphone spectrum.

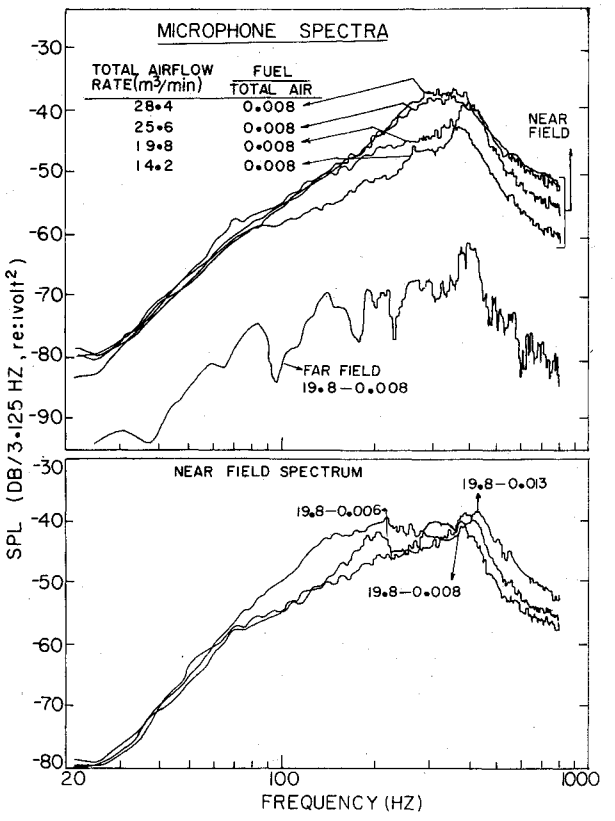

Fig. 5 Near-field spectra as a function of airflow and fuel/total air. Also shown is a typical far-field spectrum.

Experiment

Apparatus

The gas turbine combustor used in this study was described in Ref. 10. A schematic of the setup is shown in Fig. 2. A water-cooled pressure transducer capable of extracting signal above 135 dB re 2×10^{-5} N/m^2 was located on the liner wall, 92 mm from the can exit plane. A near field 1/2 in. condenser microphone was located in the can exit plane, 113 mm to the side of the liner lip. This transducer measures the can exit plane dynamic pressure as long as the frequencies are restricted to wavelengths long compared with this separation distance. Far-field microphones are employed to detect the onset of scattering from the burner hardware (nonmonopole behavior of the can exit plane) as will be explained later.

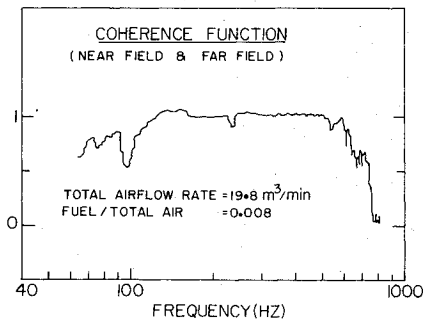

Fig. 6 Coherence between the near-and far-field microphones.

All signals are recorded on FM tape for later digital Fourier analysis. The primary items of interest are spectral shapes and coherence analysis. Calibration procedures are therefore unimportant, except to be satisfied that the microphones are behaving linearly in voltage output vs dynamic pressure level.

Results

Figure 3 displays the spectra obtained by fixed bandwidth frequency analysis of the interior microphone signal. Shown are the runs at extreme ends of the airflow and fuel/air ratio matrix. In all cases there are two regimes to the spectra. Below about 200 Hz the spectra are quite flat. Above this value the spectra undergo a hump. The upper frequency limit was chosen as 800 Hz, for reasons to be apparent later. Depending upon fuel/air ratio (speed of sound) a weak quarter wave resonance is seen in all curves in the viscinity of 400 Hz.

In contrast, look at Fig. 4 which displays a typical near-field microphone spectrum (although here a wider frequency range has been considered). At low frequency the spectrum falls off at roughly 13 dB/octave whereas the interior microphone measured a flat spectrum. By way of interest, Fig. 4 shows the 1/4, 3/4, and 5/4 wave resonance peaks. The major point is, however, that the near-field spectrum has behavior similar to the interior microphone spectrum only above about 200 Hz. More documentation on this effect is shown by the several near field spectra in Fig. 5. Also shown is a typical far-field microphone spectrum which is similar in shape to the near-field spectra, except that ground reflection effects are seen in the spectrum.

Now consider Fig. 6 which shows the near-to far-field coherence which is high (nearly perfect coherence) over the range 100-600 Hz and is acceptably high even below 100 Hz. As long as the frequency is sufficiently low that the can is behaving as a monopole radiator the far field is quite coherent with the near field even in the presence of ground reflections; this occurs because ground reflections cause only a linear transform operation on the near field signal to recover the far-field signal. Furthermore, in the frequency domain, the distance traveled to the far-field microphone only introduces a phase lag, again a linear transform operation which cancels out in coherence analysis. Above 600 Hz one concludes that scattering from the burner hardware is such that monopole behavior is destroyed; a single point measurement in the near field is insufficient to describe the total characteristics of the far-field radiation. Consequently, below 600 Hz a near-field measurement is adequate to describe the spectrum of the ultimately radiated sound power, and attention is focused only below 600 Hz.

Now view Fig. 7 which portrays the coherence between the interior and near-field microphones for several run conditions. The coherence behavior is the same for all runs; it is above 0.5 between about 150 Hz and 600 Hz and is nearly unity over the range 200-500 Hz. As frequency drops below 150 Hz the coherence drops to nearly zero. The interpretation of these results is as follows. a) a source other than combustion noise is dominating the interior microphone measurement at frequencies below 150 Hz, b) because of the

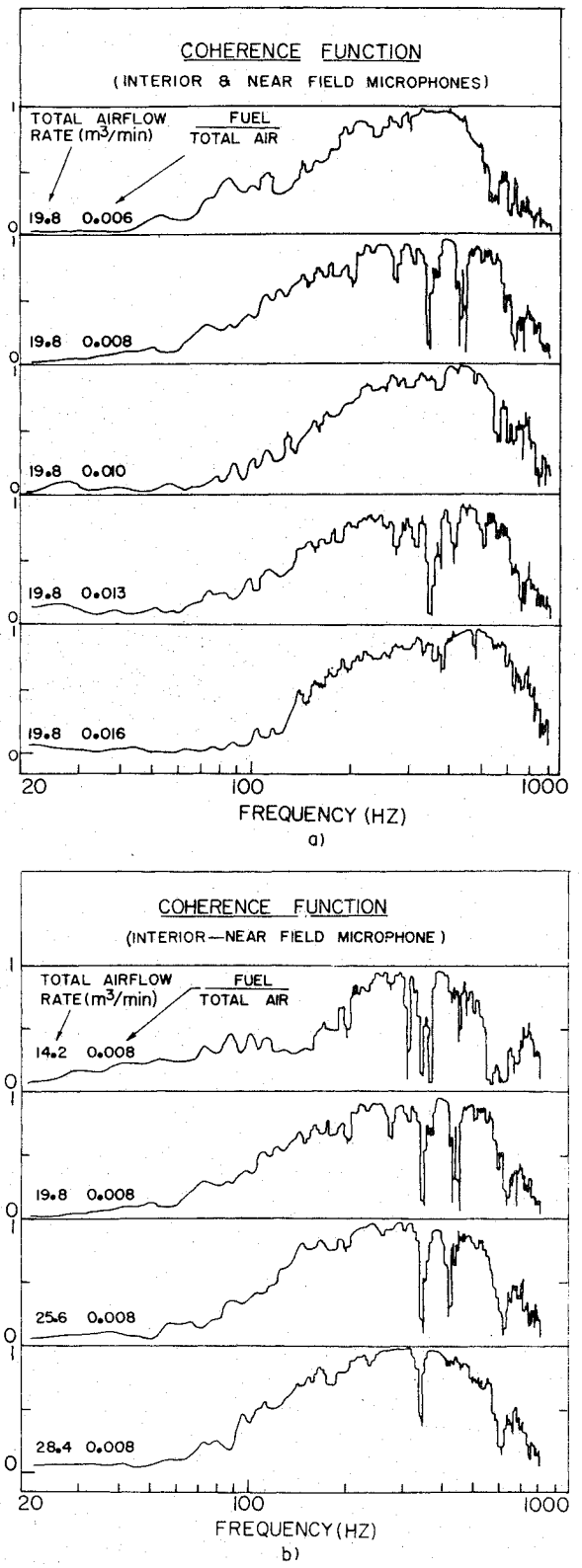

Fig. 7 Coherence between the interior and exterior microphones for several run conditions: a) Varying fuel-air ratio and fixed airflow rate; b) Varying airflow rate and fixed fuel-air ratio.

above analysis and the noncorrespondence of the spectral shapes of the two microphones at low frequency the other noise source is hydrodynamic noise caused by the vortical turbulent motions and those motions do not provide propagational sound and c) above 600 Hz the low coherence is caused by the failure of a single point measurement in the near field to characterize the entire radiation pattern; the monopole radiation pattern has ceased. The drop in the near-

field spectrum at low frequency is faster than a dropoff proportional to frequency alone, indicating that $\dot{Q}_\omega$ is falling off at roughly 6-7 dB/octave below about 300 Hz. This appears to be the primary reason for the takeover of hydrodynamic pseudosound at low frequency.

Figure 7 also shows sharp drops in coherence at some frequencies. A look at the internal spectra reveals sharp changes at these corresponding frequencies whereas the near-field spectra are smooth. This leads to the suspicion that either spurious electronic noise associated with the internal pressure transducer instrumentation or mounting of the transducer might have added some contributions to the internal signal at these frequencies.

Discussion

The results presented here can clearly be expected to be apparatus-dependent, especially with regard to the frequency at which hydrodynamic noise and combustion noise are equivalent at an interior location. The only contention here is that generally such a transition at some frequency may be expected. In the experiment here there were only two basic noise sources – flow noise and combustion noise. In an installed configuration at least two other combustor-turbine interaction noises will come into the picture to confuse the results; there will be entropy noise[11] and vorticity-nozzle interaction noise,[12] both of which will cause propagational noise and which will be sensed by both interior and exterior microphones. These sources have been avoided here by directly discharging to the atmosphere.

A major point to be stressed is that combustion noise may be present in the far-field signature even if there is little coherence between internal and external microphones. This was precisely the case at low frequency in these experiments. Consequently, some care in experiment design in installed configuration is required to determine the amount of pseudosound in the combustor as compared with propagational sound.

In the experiments here it was fortunate that the frequency content of combustion noise was low enough and the burner size was small enough that a) the plane wave mode dominated the interior acoustics, and b) the can radiated basically as a monopole over the frequency range that contained most of the combustion noise. Severe complications in interpretation can be expected if this is not the case.

Acknowledgment

This work was supported by NASA under grant number NSG 3015 and it is gratefully acknowledged.

References

[1] Abdelhamid, A.N., Harrje, D.T., Plett, E.G., and Summerfield, M., "Noise Characteristics of Combustion Augmented Jets at Midsubsonic Speeds," *AIAA Journal,* Vol. 12, March 1974, pp. 336-342.

[2] Gerend, R.P., Kumasaka, H.A., and Roundhill, J. P., "Core Engine Noise," *AIAA Progress in Astronautics and Aeronautics; Aerocaustics: Jet and Combustor Noise; Duct Acoustics,* Vol. 37, Editor: Henry T. Nagamatsu; Associate Editors: Jack V. O'Keefe and Ira R. Schwartz, MIT Press, Cambridge, Mass., 1975, pp. 305-326.

[3] Plett, E.G., Teshner, M.D., and Summerfield, M., "Combustion Geometry and Combustion Roughness Relation to Noise Generation," *Second Interagency Symposium on University Research in Transportation Noise,* Vol. 11, 1974, pp. 723-729.

[4] Bendat, J.S. and Piersol A.G., *Random Data: Analysis and Measurement Techniques,* Wiley, New York, 1971, p. 32.

[5] Strahle, W.C. and Shivashankara, B.N., "A Rational Correlation of Combustion Noise Results from Open Turbulent Flames," *Fifteenth Symposium (International) on Combustion,* The Combustion Institute, Pittsburgh, Pa., 1975, pp. 1379-1388.

[6] Chiu, H.H. and Summerfield, M., "Theory of Combustion Noise," *Acta Astronautica,* Vol. 1, 1974, pp. 967-984.

[7] Wahbah, M.M. and Strahle, W.C., "A New Method for Solving Problems of Sound Radiation for the Case of Low Mach Number," *AIAA Journal,* Vol. 15, 1977, pp. 553-560.

[8] Janardan, B.A., Daniel, B.R., and Zinn, B.T., "Characteristics of Response Factors of Coaxial Gaseous Rocket Injectors," NASA CR-134 788, 1975.

[9] Levine, H. and Schwinger, J., "On the Radiation of Sound from an Unflanged Circular Pipe," *Physical Review,* Vol. 37, 1948, pp. 383-406.

[10] Strahle, W.C. and Shivashankara, B.N., "Combustion Generated Noise in Gas Turbine Combustors," *Engineering for Power,* Vol. 98, 1976, pp. 242-246.

[11] Cumpsty, N.A., "Excess Noise from Gas Turbine Exhausts," ASME Paper 75-GT-61, 1975.

[12] Pickett, G.F., "Core Engine Noise due to Temperature Fluctuations Convecting through Turbine Blade Rows," *AIAA Progress in Astronautics and Aeronautics: Aeroacoustics: Jet and Combustor Noise; Duct Acoustics,* Vol. 37, Editor: Henry T. Nagamatsu; Associate Editors: Jack V. O'Keefe and Ira R. Schwartz, MIT Press, Cambridge, Mass., 1975, pp. 589-608.